RESPONSE TO REFEREES

Ms. Ref. No.: Egusphere-2025-2438

Title: Non-Stationary Dynamics of Compound Climate Extremes: A WRF-CMIP6-GAMLSS Framework for Risk Reassessment in Southeastern China

To Anonymous Referee #2

We sincerely appreciate your thorough and constructive comments, which have been instrumental in improving our manuscript. We also apologize for the lack of clarity in the introduction and methodology sections of the manuscript, and we assure you that these issues will be addressed in the revised version. Please find the detailed point-by-point responses below.

Major Comments:

1.Throughout the manuscript (and also in the title), the authors state that this study addresses the 'risk' of CCEs. As risk assessment typically involves an (monetary) impact analysis (see e.g. UNDRR (2007) for the definition of natural hazard risk), it may be more accurate to frame the study in terms of frequency changes or recurrence, which the authors mentioned somewhere in the manuscript. Therefore, I recommend carefully reviewing and revising all uses of "risk" or "risk assessment" to avoid overstating the study's scope.

-Answer: We fully agree with and appreciate your suggestion regarding the use of the term "risk." As the reviewer pointed out, risk assessment typically involves an analysis of impacts, particularly economic or social impacts. From the perspective of disaster-inducing factors (hazard), we have not delved into analyzing the exposure of disaster-bearing bodies (such as society, ecosystems, etc.) and their capacity to withstand these impacts. Therefore, in this context, the term "risk" is indeed not entirely appropriate. Consequently, we plan to revise the title and related statements in the revised manuscript to more accurately reflect the actual content and scope of our study. Specifically, we will remove the phrase "Risk Reassessment" from the title, resulting in the revised title: Non-Stationary Dynamics of Compound Climate Extremes: A WRF-CMIP6-GAMLSS Framework for Southeastern China.

2.While research gaps are introduced in L60-62, they require clearer identification. There are a number of studies looking into the frequency changes in compound events, both in China and other parts of the world. To name a few: Zscheischler et al. (2018), Fang et al. (2025) npj climate and atmospheric science, Wu et al. (2023) Earth's Future, Ridder et al. (2022) npj climate and atmospheric science, and so on. How does the present study compare or advance

beyond these works?

-Answer: Thank you for your valuable comment. We appreciate your suggestion and will will add a comparison with previous studies to highlight how the present study advances beyond these works and emphasizes its unique contributions in the revised manuscript.

Recent studies have increasingly focused on compound climate extremes (CCEs), highlighting their growing significance in the context of climate change. Zscheischler et al. (2018) were the first to clearly define the concept of compound events, emphasizing how the interaction of multiple climate and meteorological drivers can amplify extreme impacts. Building on this, Ridder et al. (2022) conducted the first global-scale assessment of the changes in compound events, specifically examining the co-occurrence of heatwaves and drought, extreme winds, and precipitation. Wu et al. (2023) revealed that under warming conditions, the risks associated with global compound pluvial–hot extreme events are projected to be significantly greater in the future than those observed during the historical period. Fang et al. (2025) investigated the future changes of sequential heatwaves and precipitation events (SHP) as well as concurrent drought and heatwave events (CDH) in China, with projections indicating an increase in both the frequency and intensity of these events.

While large-scale studies play a crucial role in advancing our understanding of global climate change and extreme events, their practical relevance for disaster risk management and adaptation strategies in medium- and small-scale regions is relatively limited due to their lower spatial and temporal resolution. To overcome this constraint, dynamical downscaling, which utilizes nested high-resolution regional climate models (RCMs), provides a critical technical pathway to investigate climate response mechanisms at fine-scales (Tapiador et al., 2020; Rahimi et al., 2024). In this context, over the past decade, an increasing number of studies have begun to use RCMs to obtain high-resolution climate information. Bozkurt et al. (2019) used the Regional Climate Model, version 4 (RegCM4), to evaluate the spatiotemporal variations of temperature and precipitation over the Pacific coast and the Andes Mountains. The results indicated that increasing the resolution effectively eliminates simulation errors caused by complex topography. McCrary et al. (2020) used multiple RCMs from the North American Coordinated Regional Downscaling Experiment (NA-CORDEX) to predict future snow changes in North America. They found that, particularly in high-elevation areas, the percentage of snow loss projected by GCMs was significantly higher than that projected by the RCMs. As an advanced convection-permitting RCM, the WRF model significantly enhances

the simulation capability for meteorological processes at 1-10 km scales through its fully compressible, non-hydrostatic dynamic core framework (Talbot et al., 2012). This high-resolution simulation capability gives the WRF model a unique advantage in capturing small-scale meteorological phenomena. Zhou et al. (2024) developed a 9 km resolution regional reanalysis dataset covering the Tibetan Plateau based on the WRF model, and demonstrated its superior applicability compared to the fifth generation European Centre for Medium-Range Weather Forecasts Reanalysis (ERA5). Yang et al. (2024) revealed that the WRF model provides better accuracy in simulating snow depth during the cold season in high-elevation regions compared to ERA5-Land.

Additionally, traditional extreme event analyses rely on stationarity assumptions, presuming that the probability and distributional parameters of climate variables are constant (Sun et al., 2018; Nerantzaki et al., 2023). However, driven by synergistic effects of global warming and anthropogenic forcing, extremes exhibit significant shifts in distributional characteristics (Gao et al., 2018). Therefore, traditional models are not suitable for evaluating extreme changes in the changing environment. To capture these changes, many studies have applied the Generalized Additive Models for Location, Scale, and Shape (GAMLSS) (Rigby and Stasinopoulos 2005) to address non-stationary problems in hydrological and meteorological extremes, enabling updated risk analysis of evolving climate extremes (Lei et al., 2021; Shao et al., 2022; Jin et al., 2023; Li et al., 2024). ***However, existing non-stationary analyses only focus on individual extremes, and the potential non-stationarity of CCEs has not been established. The comprehensive assessment of future changes in CCEs recurrence risk within a non-stationary framework is also lacking.***

To address these research gaps, this study adopts a high-resolution approach, combining the WRF model with GAMLSS. This approach overcomes the limitations of traditional coarse-resolution models and addresses the shortcomings of stationary assumptions in analyzing compound climate extremes (CCEs). By focusing on the Minjiang River Basin (MRB), this research aims to explore four types of CCEs: hot-wet events (HW), hot-dry events (HD), cold-wet events (CW), and cold-dry events (CD). The analysis proceeds as follows (Fig. 1): Supplement Section S1 presents the validation of CMIP6bc applicability. Section 3.1 characterizes the spatio-temporal patterns of CCEs under both a middle-of-the-road scenario (SSP2-4.5) and a high-emissions scenario (SSP5-8.5). The non-stationarity detection of CCEs is described in Section 3.2. The recurrence risk changes in CCEs under non-stationary

conditions is evaluated in Section 3.3. The work establishes a scientific basis for addressing the environmental and climatic challenges posed by CCEs, thereby contributing to effective strategies for regional sustainability and climate resilience.

References

Bozkurt, D., Rojas, M., Boisier, J.P., Rondanelli, R., Garreaud, R., Gallardo, L., 2019. Dynamical downscaling over the complex terrain of southwest South America: present climate conditions and added value analysis. Clim. Dyn. 53, 6745–6767. https://doi.org/10.1007/s00382-019-04959-y

Fang, P., Wang, T., Yang, D., Tang, L., Yang, Y., 2025. Substantial increases in compound climate extremes and associated socio-economic exposure across China under future climate change. npj Clim. Atmos. Sci. 8, 17. https://doi.org/10.1038/s41612-025-00910-7

Gao, L., Huang, J., Chen, X., Chen, Y., Liu, M., 2018. Contributions of natural climate changes and human activities to the trend of extreme precipitation. Atmos. Res. 205, 60–69. https://doi.org/10.1016/j.atmosres.2018.02.006

Jin, H., Willems, P., Chen, X., Liu, M., 2023. Nonstationary flood and its influencing factors analysis in the Hanjiang River Basin, China. J. Hydrol. 625, 129994. https://doi.org/10.1016/j.jhydrol.2023.129994

Lei, X., Gao, L., Ma, M., Wei, J., Xu, L., Wang, L., Lin, H., 2021. Does non-stationarity of extreme precipitation exist in the Poyang Lake Basin of China? J. Hydrol.: Reg. Stud. 37, 100920. https://doi.org/10.1016/j.ejrh.2021.100920

Li, M., Feng, Z., Zhang, M., Yao, Y., 2024. Influence of large-scale climate indices and regional meteorological elements on drought characteristics in the Luanhe River Basin. Atmos. Res. 300, 107219. https://doi.org/10.1016/j.atmosres.2024.107219

McCrary, R.R., Mearns, L.O., Abel, M.R., Biner, S., Bukovsky, M.S., 2022. Projections of North American snow from NA-CORDEX and their uncertainties, with a focus on model resolution. Climatic Change 170, 20. https://doi.org/10.1007/s10584-021-03294-8

Nerantzaki, S.D., Papalexiou, S.M., Rajulapati, C.R., Clark, M.P., 2023. Nonstationarity in High and Low-Temperature Extremes: Insights From a Global Observational Data Set by Merging Extreme-Value Methods. Earth's Future 11, e2023EF003506. https://doi.org/10.1029/2023EF003506

Rahimi, S., Huang, L., Norris, J., Hall, A., Goldenson, N., Risser, M., Feldman, D.R., Lebo,

Z.J., Dennis, E., Thackeray, C., 2024. Understanding the Cascade: Removing GCM Biases Improves Dynamically Downscaled Climate Projections. Geophys. Res. Lett. 51, e2023GL106264. https://doi.org/10.1029/2023GL106264

Ridder, N.N., Ukkola, A.M., Pitman, A.J., Perkins-Kirkpatrick, S.E., 2022. Increased occurrence of high impact compound events under climate change. npj Clim. Atmos. Sci. 5, 3. https://doi.org/10.1038/s41612-021-00224-4

Rigby, R.A., Stasinopoulos, D.M., 2005. Generalized Additive Models for Location, Scale and Shape. J. R. Stat. Soc. Series C: Appl. Stat. 54, 507–554. https://doi.org/10.1111/j.1467-9876.2005.00510.x

Shao, S., Zhang, H., Singh, V.P., Ding, H., Zhang, J., Wu, Y., 2022. Nonstationary analysis of hydrological drought index in a coupled human-water system: Application of the GAMLSS with meteorological and anthropogenic covariates in the Wuding River basin, China. J. Hydrol. 608, 127692. https://doi.org/10.1016/j.jhydrol.2022.127692

Sun, F., Roderick, M.L., Farquhar, G.D., 2018. Rainfall statistics, stationarity, and climate change. Proc. Natl. Acad. Sci. U.S.A. 115, 2305–2310. https://doi.org/10.1073/pnas.1705349115

Talbot, C., Bou-Zeid, E., Smith, J., 2012. Nested Mesoscale Large-Eddy Simulations with WRF: Performance in Real Test Cases. J. Hydrometeorol. 13, 1421–1441. https://doi.org/10.1175/JHM-D-11-048.1

Tapiador, F.J., Navarro, A., Moreno, R., Sánchez, J.L., García-Ortega, E., 2020. Regional climate models: 30 years of dynamical downscaling. Atmos. Res. 235, 104785. https://doi.org/10.1016/j.atmosres.2019.104785

Wu, H., Su, X., Singh, V.P., 2023. Increasing Risks of Future Compound Climate Extremes With Warming Over Global Land Masses. Earth's Future 11, e2022EF003466. https://doi.org/10.1029/2022EF003466

Yang, T., Chen, X., Hamdi, R., Li, Q., Cui, F., Li, L., Liu, Y., De Maeyer, P., Duan, W., 2024. Assessment of snow simulation using Noah-MP land surface model forced by various precipitation sources in the Central Tianshan Mountains, Central Asia. Atmos. Res. 300, 107251. https://doi.org/10.1016/j.atmosres.2024.107251

Zhou, P., Tang, J., Ma, M., Ji, D., Shi, J., 2024. High resolution Tibetan Plateau regional reanalysis 1961-present. Sci. Data 11, 444. https://doi.org/10.1038/s41597-024-03282-4

Zscheischler, J., Westra, S., Van Den Hurk, B.J.J.M., Seneviratne, S.I., Ward, P.J., Pitman, A.,

AghaKouchak, A., Bresch, D.N., Leonard, M., Wahl, T., Zhang, X., 2018. Future climate risk from compound events. Nature Clim. Change 8, 469–477. https://doi.org/10.1038/s41558-018-0156-3

3.Fig. 1 outlines the key methodological steps in this study. Many unintroduced acronyms e.g. WRFOUT, CC and PBIAS are used without prior explanation, which may reduce the readability and understanding of the framework.

-Answer: Thank you for your comment. We agree with your suggestion and will revise Figure 1 in the revised manuscript to ensure better readability for the readers.

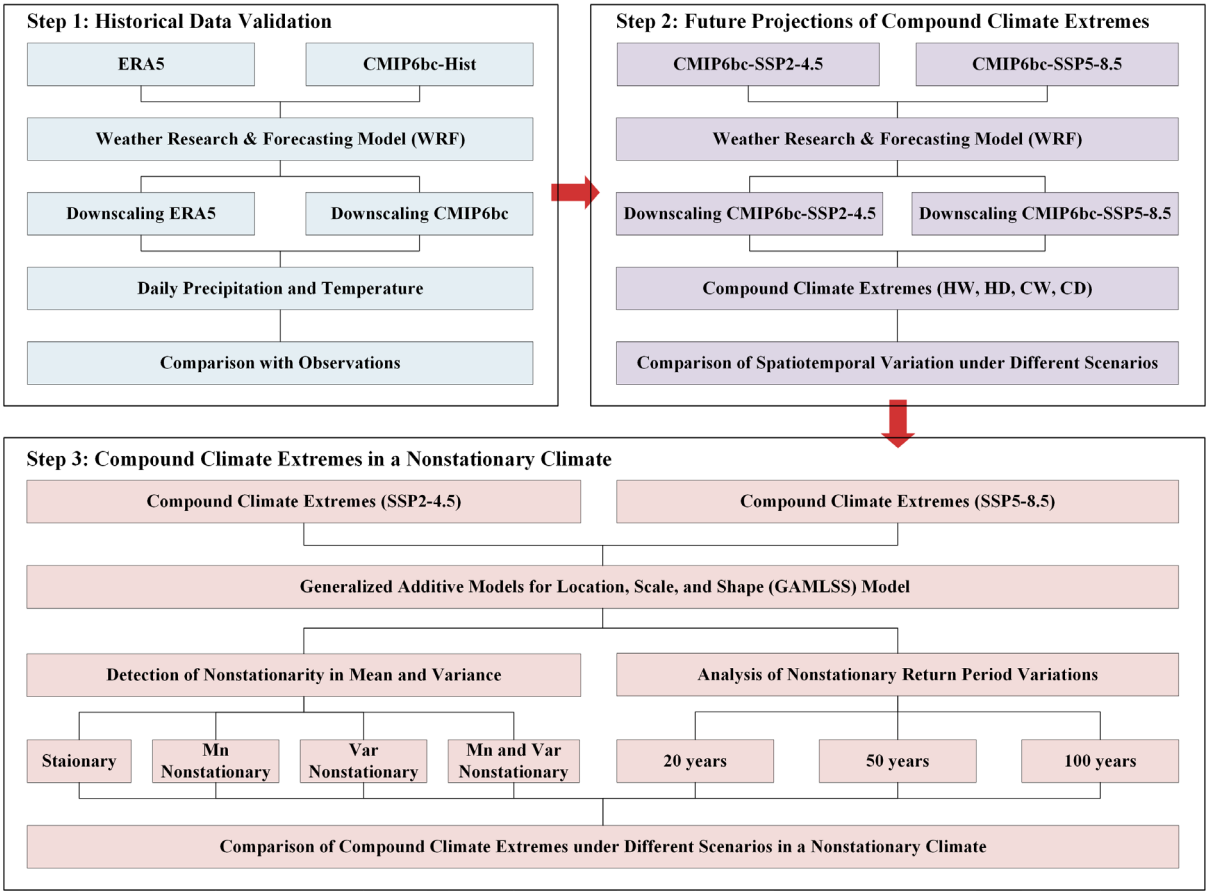

Fig. 1. Flowchart of CCEs projection in a non-stationary framework.

4.Please elaborate on the types of CCEs commonly occurring during the flood season (Line 99). Including examples of historical events would help illustrate this.

-Answer: Thank you for your constructive comment. We agree that providing more details in the revised manuscript.

The basin displays spatio-temporal heterogeneity in precipitation, with flood seasons from April to September that often accompany CCEs. Particularly in the late flood season (July to

September), the MRB experiences frequent typhoon-related compound disasters: the upper and middle reaches are commonly affected by typhoon-rainstorm-landslide events, while the lower reaches face high occurrences of typhoon-rainstorm-urban waterlogging and typhoon-rainstorm-flood events (Yang et al., 2025). In 2023, for example, Typhoon Doksuri (No. 2305) caused approximately 66,794 people to be affected in Fuzhou, the downstream city of the MRB, with direct economic losses reaching 588 million RMB (Yan et al., 2024). In addition, the region also exhibits a climate characteristic of concurrent rainfall and heat, with CCEs frequently occurring during the warm season, driven by high temperatures and heavy rainfall (Sun et al., 2025).

References

Sun, X., Tu, Y., Sun, S., Zhou, X., Jiang, L., Hao, X., Jiang, C., Gao, L., 2025. Identification and spatiotemporal characteristics of compound extreme climate events in the Minjiang River Basin. Water Resour. Hydropower Engineering 56 (3): 1-14. https://doi:10.13928/j.cnki.wrahe.2025.03.001 (In Chinese)

Yan, Y., Gao, L., Chen, R., Zhang, C., Ren, L., Zhang, X., Chen, C., 2024. Analysis of Disaster and Damage Process Caused by No. 2305 "Doksuri" Typhoon Disaster Chain in Fuzhou City. J. Catastrophology 39 (4): 228-234. https://doi: 10. 3969/j. issn. 1000-811X. 2024. 04. 033 (In Chinese)

Yang, X., Yan, Y., Zhou, X., Zhu, L., Ma, M., Zhang, J., Chen, Y., Gao, L., 2025. Risk of Compound Typhoon Disaster Chains: Insights from Southeastern China. Int. J. Disaster Risk Sci. 16, 870–887. https://doi.org/10.1007/s13753-025-00674-x

5.Section 2 provides a description of critical methodological steps of this work; however, they lack sufficient detail to fully convey its approach and practical implementation. I suggest to clarify the following concerns:

a.For validation of historical simulation results:

i.Why is the validation only focused on a 10-year period (2005–2014)?

-Answer: Thank you very much for your insightful comment. We would like to clarify that the bias-corrected CMIP6 dataset (Xu et al., 2021) we used has already been extensively validated (Jamal et al., 2023; Huang et al., 2024; Wu and Zheng, 2023). Given that the focus of our study is on assessing the non-stationary changes of future compound climate extremes (CCEs), a comprehensive and detailed evaluation of the dataset was not conducted. Additionally, running WRF simulations requires substantial computational resources—for example, simulating one

year over the MRB takes approximately 4 days on 80 CPU cores. Considering both the reliability of the dataset and the need to optimize computational resources, we select a 10-year historical period (2005–2014) as being sufficient to demonstrate the reliability of the bias-corrected data for our study purposes.

References

Huang, Y., Xue, M., Hu, X., Martin, E., Novoa, H.M., McPherson, R.A., Liu, C., Chen, M., Hong, Y., Perez, A., Morales, I.Y., Ticona Jara, J.L., Flores Luna, A.J., 2024. Increasing frequency and precipitation intensity of convective storms in the Peruvian Central Andes: Projections from convection-permitting regional climate simulations. Quart. J Royal Meteoro. Soc. 150, 4371–4390. https://doi.org/10.1002/qj.4820

Jamal, K., Li, X., Chen, Y., Rizwan, M., Khan, M.A., Syed, Z., Mahmood, P., 2023. Bias correction and projection of temperature over the altitudes of the Upper Indus Basin under CMIP6 climate scenarios from 1985 to 2100. J. Water Clim. Change 14, 2490–2514. https://doi.org/10.2166/wcc.2023.180

Wu, L., Zheng, H., 2023. Regional Climate Effects of Irrigation under Central Asia Warming by 2.0 °C. Remote Sens. 15, 3672. https://doi.org/10.3390/rs15143672

Xu, Z., Han, Y., Tam, C.-Y., Yang, Z.-L., Fu, C., 2021. Bias-corrected CMIP6 global dataset for dynamical downscaling of the historical and future climate (1979–2100). Sci. Data 8, 293. https://doi.org/10.1038/s41597-021-01079-3

ii. Why would the ERA5 serve as the benchmark not the observed data (L113-115)?

-Answer: Thank you for your question. We would like to clarify that, in fact, we have three sets of data: observed data, WRF-ERA5, and WRF-CMIP6bc. ERA5, as a widely used WRF-driven dataset, is utilized here as a reference for the simulation results. Indeed, the actual validation data comes from the meteorological station observations (Figure S1).

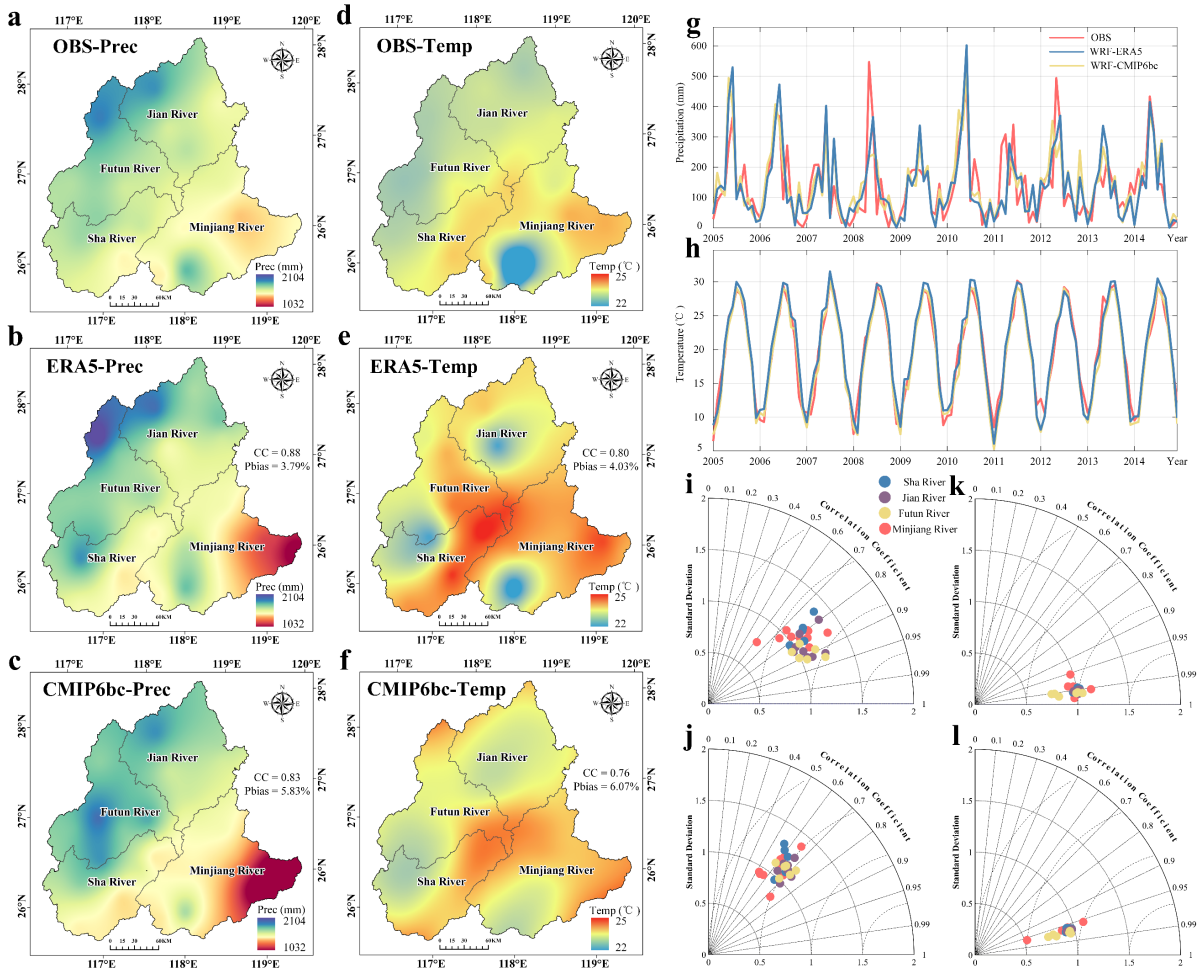

Figure S1. Evaluation of WRF-simulated precipitation and temperature over the MRB (2005-2014). Spatial patterns of precipitation (a–c), temperature (d–f). Temporal evolution of precipitation (g) and temperature (h). Panels (i–l) present sub-basin comparisons of precipitation and temperature from ERA5 (i, k) and CMIP6bc (j, l).

iii. How were the spatial results constructed from the observed data at 30 stations?

-Answer: Thank you for your question. The spatial distribution results of the CCEs were constructed by performing spline interpolation on the observed data from the 30 stations in the MRB using Arc Geographic Information System (ArcGIS). To eliminate the interpolation errors, we extracted the nearest WRF grid points for each meteorological station and compared

them by plotting a Taylor diagram. We believe that using both spatial interpolation and point-to-point validation can effectively reduce uncertainty in the results. We will provide a more detailed explanation of this approach in the revised manuscript.

iv. Please define in the manuscript what CC and PBIAS mean, and clarify whether they represent averages across all grid cells.

-Answer: Thank you for your comment. We will add definitions of the evaluation metrics in the revised manuscript (Table 2). We would also like to clarify that in the spatial maps, CC and PBIAS represent the averages across all stations, whereas in the Taylor diagrams, CC, RMSE, and STD are calculated based on the nearest WRF grid point to each station.

Table 2 Definition of evaluation criteria.

Metric	Formula	Optimal value	Range
CC	$CC = \frac{\sum_{i=1}^{n}(O_i - \overline{O_i})(M_i - \overline{M_i})}{\sqrt{\sum_{i=1}^{n}(O_i - \overline{O_i})^2}\sqrt{\sum_{i=1}^{n}(M_i - \overline{M_i})^2}}$	1	(0, 1)
PBIAS	$PBIAS = \sum_{i=1}^{n} \frac{M_i - O_i}{O_i}$	0	(-∞, +∞)
RMSE	$RMSE = \sqrt{\frac{1}{n}\sum_{i=1}^{n}(M_i - O_i)}$	0	(0, +∞)
STD	$STD = \sqrt{\frac{1}{n}\sum_{i=1}^{n}(O_i - \bar{O})^2}$	0	(0, +∞)

Notes: Where O_i presents hydrometeorological data at the i station, M_i presents data at the WRF grid point closest to the i station, n is the numbers of stations.

v. What are subplots a-f in Figure S1 based on? The mean value per grid over the 10-year historic period? Please add necessary details on what you are comparing.

Thank you for your question. Subplots a–f in Figure S1 represent the interpolated annual mean values at each meteorological station and the nearest WRF grid point over the 10-year historical period. We will add this description in the revised manuscript.

vi. Is there also an explanation on those misestimated CMIP6bc temperatures? And why are the results particularly worse in the downstream sub-basin of the MRB?

-Answer: Thank you for your question. We will provide an explanation for this issue in the supplement.

The WRF model's simulation of temperature in complex terrain is mainly influenced by factors such as radiation transfer, surface type, and meteorological initial conditions (Jiménez-Esteve et al., 2018; Liu et al., 2019; Lu et al., 2021). High-altitude areas typically experience

stronger radiation effects, especially in mountainous regions with thinner atmospheres. The WRF model may have errors in simulating radiation transfer, leading to temperatures in high-altitude areas being lower than actual conditions (Varga et al., 2020). In addition, the downstream area of the MRB is an urban agglomeration, where urban areas typically experience stronger radiation and heat accumulation effects. These effects may not be fully accounted for in the model, leading to simulated temperatures being higher than actual conditions (Li et al., 2014; Chen et al., 2025). Ntoumos et al. (2023) also revealed that the WRF model tends to overestimate the maximum temperatures and underestimate the minimum temperatures, with the errors being closely related to the geographic location.

References

Chen, G., Mei, S.-J., Hang, J., Li, Q., Wang, X., 2025. URANS simulations of urban microclimates: Validated by scaled outdoor experiments. Build. Environ. 272, 112691. https://doi.org/10.1016/j.buildenv.2025.112691

Jiménez-Esteve, B., Udina, M., Soler, M.R., Pepin, N., Miró, J.R., 2018. Land use and topography influence in a complex terrain area: A high resolution mesoscale modelling study over the Eastern Pyrenees using the WRF model. Atmos. Res. 202, 49–62. https://doi.org/10.1016/j.atmosres.2017.11.012

Li, M., Feng, Z., Zhang, M., Yao, Y., 2024. Influence of large-scale climate indices and regional meteorological elements on drought characteristics in the Luanhe River Basin. Atmos. Res. 300, 107219. https://doi.org/10.1016/j.atmosres.2024.107219

Liu, L., Ma, Y., Menenti, M., Zhang, X., Ma, W., 2019. Evaluation of WRF Modeling in Relation to Different Land Surface Schemes and Initial and Boundary Conditions: A Snow Event Simulation Over the Tibetan Plateau. J. Geophys. Res.: Atmos. 124, 209–226. https://doi.org/10.1029/2018JD029208

Lu, S., Guo, W., Xue, Y., Huang, F., Ge, J., 2021. Simulation of summer climate over Central Asia shows high sensitivity to different land surface schemes in WRF. Clim. Dyn. 57, 2249–2268. https://doi.org/10.1007/s00382-021-05876-9

Ntoumos, A., Hadjinicolaou, P., Zittis, G., Constantinidou, K., Tzyrkalli, A., Lelieveld, J., 2023. Evaluation of WRF Model Boundary Layer Schemes in Simulating Temperature and Heat Extremes over the Middle East–North Africa (MENA) Region. J. Appl. Meteorol. Clim. 62, 1315–1332. https://doi.org/10.1175/JAMC-D-22-0108.1

Varga, Á.J., Breuer, H., 2020. Sensitivity of simulated temperature, precipitation, and global

radiation to different WRF configurations over the Carpathian Basin for regional climate applications. Clim. Dyn. 55, 2849–2866. https://doi.org/10.1007/s00382-020-05416-x

b. I suggest to swap Sect. 2.3 and 2.4, since you first run the model and then extract CCEs from the model results.

-Answer: Thank you for your constructive suggestion. We agree with your point and will swap Sections 2.3 and 2.4 in the revised manuscript

i. When identifying the CCE events, did you do it independently for each grid? What are the spatiotemporal definitions of CCEs?

-Answer: Thank you for your question. In response to your inquiry, indeed, when identifying compound climate extremes (CCEs), we performed calculations independently for each grid point. Specifically, we sorted the precipitation and temperature data for each grid point over a 40-year period and defined extreme events based on the 10th and 90th percentiles. The methodology we used is based on the approach outlined by Wang et al. (2024), and the calculations are conducted using independent thresholds for each grid point, without considering co-occurrence of extreme events across multiple grid points. As for the issue of spatially compound disasters, I will address that in my response to the next question.

References

Wang, Yingshan, Sun, W., Huai, B., Wang, Yuzhe, Ji, K., Yang, X., Du, W., Qin, X., Wang, L., 2024. Comparison and evaluation of the performance of reanalysis datasets for compound extreme temperature and precipitation events in the Qilian Mountains. Atmos. Res. 304, 107375. https://doi.org/10.1016/j.atmosres.2024.107375

ii. Did you consider the spatially compound events, i.e. the same CCE event occur at multiple locations simultaneously? If not, please discuss if the proposed approach may double count CCEs and how does this affect your conclusion.

-Answer: Thank you for your question. You've raised a very important point, and we fully understand your concern about whether the simultaneous occurrence of the same compound climate extreme event (CCE) across multiple grid points might lead to double counting, potentially affecting the reliability of the results. In response, we would like to clarify that when calculating the compound extreme indices, we perform the calculations independently for each grid point. For example, in Fig. 3, subplots a-j show the annual mean spatial distribution of each type of CCE for each grid point over the 40-year period, rather than the total sum. Therefore, even if the same event occurs at multiple grid points simultaneously, this will not

lead to double counting (For example, even if the same CCE occurs on the same day at two grid points, it will still be counted as one day after averaging.). Similarly, for subplots k-o, the time series variations are averaged across the grid points, representing the mean values of the entire basin, not the total sum, so there is no issue of double counting in these results either.

Nevertheless, we appreciate the insightful nature of your comment. Spatially compound events are a more complex concept, and we intend to conduct separate analyses for such cases in future studies.

c.Please include the results of your sensitivity experiments (L130) in the supplementary materials.

-Answer: Thank you for your suggestion. We will include the results of the sensitivity experiments in the supplementary materials.

In our previous study, we conducted a detailed sensitivity analysis and optimization of parameterization schemes specifically for the MRB (Lin et al., 2023). We focused on two schemes that have the most significant impact on precipitation: microphysics and cumulus convection. By cross-combining these schemes, we developed 16 combinations (as shown in Table S2) and assessed their performance in simulating precipitation across different magnitudes. Through a comprehensive evaluation of the temporal (Fig. S1 and Fig. S3) and spatial (Fig. S3 and Table S3) characteristics, we determined that the 9th configuration (Lin and NT) is the most suitable for simulating extreme precipitation events in the MRB. As a result, this configuration was adopted in the present study to ensure the most accurate simulation of extreme precipitation events in this region.

Table S2 Parameterization scheme combinations design.

Combinations	Microphysics scheme (MP)	Cumulus scheme (CU)
EXP1	WSM6	Betts-Miller-Janjic (BMJ)
EXP2	WSM6	Betts-Miller-Janjic (BMJ)
EXP3	WSM6	Betts-Miller-Janjic (BMJ)
EXP4	WSM6	Betts-Miller-Janjic (BMJ)
EXP5	WDM6	Kain-Fritsch (KF)
EXP6	WDM6	Kain-Fritsch (KF)
EXP7	WDM6	Kain-Fritsch (KF)
EXP8	WDM6	Kain-Fritsch (KF)
EXP9	Purdue Lin (Lin)	New Tiedtke (NT)
EXP10	Purdue Lin (Lin)	New Tiedtke (NT)

EXP11	Purdue Lin (Lin)	New Tiedtke (NT)
EXP12	Purdue Lin (Lin)	New Tiedtke (NT)
EXP13	Thompson	Grell-Devenyi (GD)
EXP14	Thompson	Grell-Devenyi (GD)
EXP15	Thompson	Grell-Devenyi (GD)
EXP16	Thompson	Grell-Devenyi (GD)

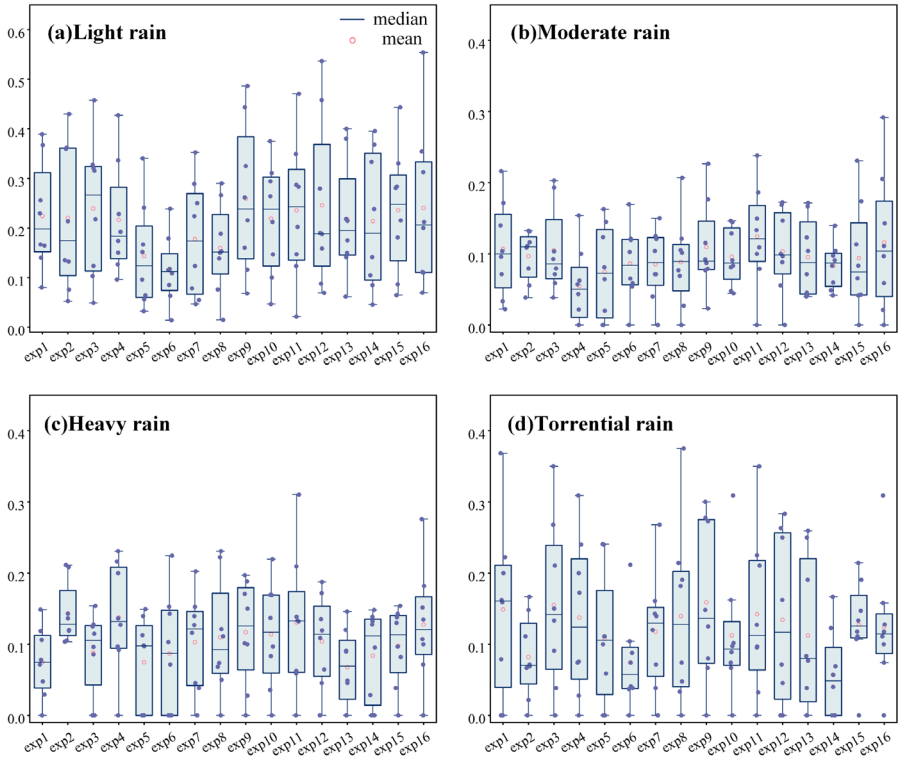

Fig. S2. Box plot of TS scores for 24-hour accumulated precipitation simulated by WRF.

Table S3 Evaluation metrics for total accumulated precipitation

Combination	TS (light)	TS (moderate)	TS (heavy)	TS (torrential)	$\overline{TS}$	$\overline{POD}$	$\overline{FAR}$
EXP1	0.22	0.11	0.07	0.15	0.14	0.24	0.71
EXP2	0.22	0.10	0.14	0.08	0.14	0.24	0.69
EXP3	0.24	0.11	0.09	0.16	0.15	0.27	0.66
EXP4	0.22	0.05	0.14	0.14	0.14	0.25	0.70
EXP5	0.14	0.07	0.07	0.11	0.10	0.16	0.71
EXP6	0.12	0.09	0.09	0.07	0.09	0.15	0.74
EXP7	0.18	0.09	0.10	0.12	0.12	0.20	0.64
EXP8	0.16	0.09	0.11	0.14	0.12	0.19	0.68
EXP9	0.26	0.11	0.12	0.16	0.16	0.29	0.66
EXP10	0.22	0.10	0.11	0.11	0.14	0.24	0.74
EXP11	0.24	0.12	0.13	0.14	0.16	0.23	0.55

EXP12	0.25	0.10	0.10	0.13	0.15	0.24	0.71
EXP13	0.22	0.10	0.07	0.11	0.12	0.21	0.67
EXP14	0.21	0.08	0.08	0.06	0.11	0.20	0.74
EXP15	0.24	0.09	0.10	0.13	0.14	0.25	0.70
EXP16	0.24	0.12	0.13	0.12	0.15	0.26	0.67

Note: TS (light rain, moderate rain, heavy rain, torrential rain) refers to the average of daily 24-hour accumulated precipitation. $\overline{TS}$、$\overline{POD}$、$\overline{FAR}$ represent the average values of the scores for the four precipitation levels.

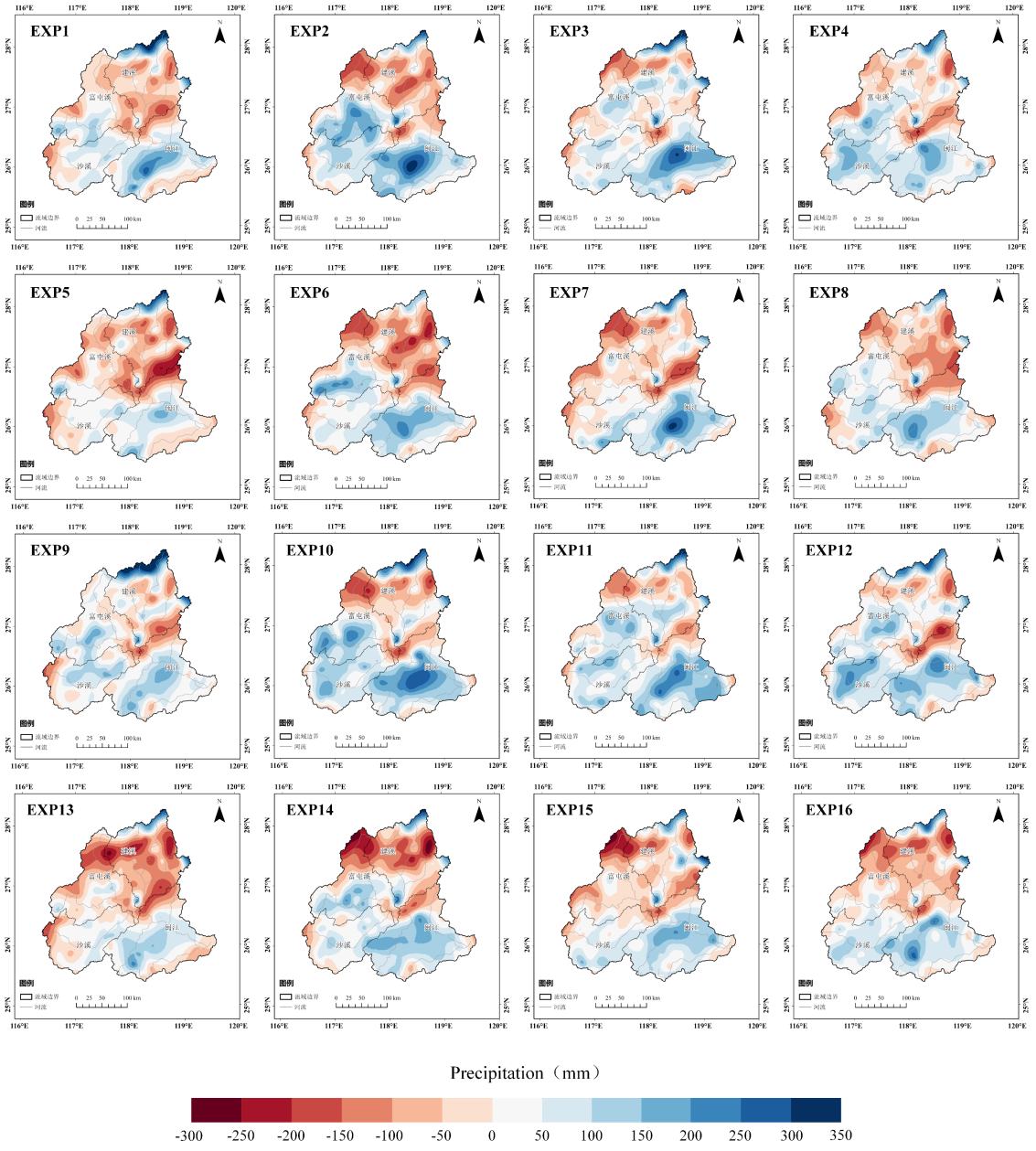

Fig. S3. Spatial distribution of biases of total accumulated precipitation from WRF parametrization scheme sensitivity experiments.

References

Lin, S., Zhang, Y., Sun, S., Guan, X., Jiang, C., Gao, L., 2023. Sensitivity study of WRF parameterization schemes and initial fields on simulation of rainstorm in the Minjiang River basin. Pearl River 44(10): 35-46+61. https://doi: 10.3969/j.issn.1001-9235.2023.10.004 (in Chinese)

d.While Sect. 2.4.2 introduces the GAMLSS model, it lacks the detail on how WRF results are used in this model. The authors may include suitable examples when explaining the proposed approach. For example, how are the daily temperature and precipitation or the identified CCEs used in the model?

-Answer: Thank you for your suggestion. In our study, the output from the WRF model (precipitation and temperature) is used as meteorological variables to identify and calculate compound climate extreme events (CCEs), including hot-wet events (HW), hot-dry events (HD), cold-wet events (CW), and cold-dry events (CD). After calculating the CCEs for each grid point, these events are input into the GAMLSS model for further analysis. In the GAMLSS model, time (year) is used as the independent variable (x), and the number of days per year for each type of CCE is treated as the dependent variable (y), thereby enabling the calculation of the non-stationary characteristics of each CCE.

e.L158-159: "we fit non-stationary GAMLSS models with two parameters (mean, variance) and four parameters (mean, variance, skewness, kurtosis) at each grid point, selecting the optimal model for subsequent analysis." What is the difference between the mean and variance in the first mention (two parameters) and in the following (four parameters)? And how are the changes between the current and future CCE frequency estimated and in what unit/form?

-Answer: We appreciate the reviewer's attention to this point. We employed two types of GAMLSS models to capture potential changes in the distribution of meteorological variables. The first is the traditional two-parameter location–scale model (mean μ and variance σ), which assumes a fixed distributional shape. The second is a more flexible four-parameter location–scale–shape model (mean μ, variance σ, skewness ν, and kurtosis τ), which allows the distributional shape to vary over time. These extended distributions retain the mean and variance parameters but include two extra shape parameters to capture asymmetry and tail behavior. We evaluate these models by comparing their goodness of fit and then select the model that best represents the data distribution for subsequent analyses. Additionally, skewness and kurtosis are unitless statistics that measure the asymmetry and tail thickness of the data

distribution, respectively. The unit of frequency change is days per decade, and it was calculated by using linear regression based on annual data to estimate the trend of frequency change.

6.Please describe in the methodology how metrics such as annual event distribution, seasonal variations, and non-stationary characteristics were calculated.

-Answer: Thank you for your suggestion. We will include this additional information in the methodology section. In calculating the interannual and seasonal variations of CCEs, we used different threshold values. Specifically, for interannual variation, we sorted the precipitation and temperature data over a 40-year period and determined the thresholds based on the 10th and 90th percentiles to identify CCEs. For seasonal variations, we separately extracted the precipitation and temperature data for the summer (JJA) and winter (DJF) seasons, applying the same sorting method to calculate the respective thresholds, thus analyzing the distribution characteristics of CCEs for each season.

Regarding the calculation of stationarity, we employed the GAMLSS to fit the changes in the mean and variance of CCEs. To assess their stationarity over time, we consider the CCEs to be stationary if both the mean and variance remain stable. If either the mean or variance shows significant variation, the CCEs are considered non-stationary.

7.In Fig. 3 (a-j), do the annual spatial values refer to the mean yearly event number over 2025-2065? What does d/10a mean?

-Answer: Thank you for your question. We apologize for the previous lack of clarity in our description. In Fig. 3 (a-j), the annual spatial values represent the mean yearly event number over the period 2025-2065. Regarding the term "d/10a," we will revise it to "days per decade" to ensure clearer understanding.

8.When looking at the temporal changes in CCEs (Fig. 3 k-o), it is interesting to see the projections for two SSPs sometimes show a completely different year-to-year trend. For example, for hot-dry events, the value in blue increases from 2032 to 2033 while the red one decreases. There are also similar discrepancies for different years and different compound events. Is there an explanation for this?

-Answer: Thank you for pointing out this important issue. The inconsistency, or even opposite trends, of extreme events in some regions under the SSP2-4.5 and SSP5-8.5 pathways in climate simulations is reasonable and expected. This is mainly due to the dominant role of internal climate variability at the regional scale. Although the greenhouse gas forcing in SSP5-

8.5 is stronger, the global warming and atmospheric circulation responses (such as changes in jet stream positions or shifts in storm tracks) caused by it differ spatially from those in SSP2-4.5. These differences interact in complex ways with decadal-scale internal oscillations, such as the Pacific Decadal Oscillation (PDO) or the Atlantic Multidecadal Oscillation (AMO). During specific periods and in certain regions, these strong natural variability signals may temporarily mask or even reverse the long-term trends driven by external forcing, leading to different short-term evolution paths under the two scenarios. Additionally, similar cases have been observed in previous studies (Fig. 5 (Wu et al., 2023); Fig. 7 (Ren et al., 2023); Fig.2 (Fang et al., 2025)), demonstrating that short-term variability under different emission scenarios is quite common.

References

Fang, P., Wang, T., Yang, D., Tang, L., Yang, Y., 2025. Substantial increases in compound climate extremes and associated socio-economic exposure across China under future climate change. npj Clim. Atmos. Sci. 8, 17. https://doi.org/10.1038/s41612-025-00910-7

Ren, J., Huang, G., Zhou, X., Li, Y., 2023. Downscaled compound heatwave and heavy-precipitation analyses for Guangdong, China in the twenty-first century. Clim. Dyn. 61, 2885–2905. https://doi.org/10.1007/s00382-023-06712-y

Wu, X., Yang, Y., Jiang, D., 2023. Dramatic increase in the probability of 2006-like compound dry and hot events over Southwest China under future global warming. Weather Clim. Extremes 41, 100592. https://doi.org/10.1016/j.wace.2023.100592

9.Similar to my earlier comment, if you did not consider the same CCE occurring across cells. Be careful with drawing conclusions from the averaged days as you may double count some events.

-Answer: Thank you very much for your question. The response to this issue is the same as for question 5. b. II.

We perform the calculations independently for each grid point. For example, in Fig. 3, subplots a-j show the annual mean spatial distribution of each type of CCE for each grid point over the 40-year period, rather than the total sum. Therefore, even if the same event occurs at multiple grid points simultaneously, this will not lead to double counting (For example, even if the same CCE occurs on the same day at two grid points, it will still be counted as one day after averaging.). Similarly, for subplots k-o, the time series variations are averaged across the

grid points, representing the mean values of the entire basin, not the total sum, so there is no issue of double counting in these results either.

Nevertheless, we appreciate the insightful nature of your comment. Spatially compound events are a more complex concept, and we intend to conduct separate analyses for such cases in future studies.

10.For showing the seasonal variations, I was wondering would it be better to compare the event number/frequency between different seasons for a given CCE, instead of presenting results for all four CCEs for a given season.

-Answer: Thank you for your suggestion. We will make the adjustment as you recommended in the revised manuscript.

11.How were the return periods calculated?

-Answer: Thank you for your question. In this study, the calculation of return periods is based on the threshold exceedance method, which fundamentally links the return period to the frequency of extreme events. Specifically, we extracted all extreme events from the historical data that exceeded the predetermined threshold and constructed a sequence of their "frequency (days per year)." By analyzing this frequency and fitting the optimal distribution (Gao et al., 2018), we calculated the "frequency for a 10-year return period" (for example, X days per year). This means that a "10-year return period event" refers to the frequency of such an event occurring. We will clarify this concept further in the revised manuscript.

References

Gao, L., Huang, J., Chen, X., Chen, Y., Liu, M., 2018. Contributions of natural climate changes and human activities to the trend of extreme precipitation. Atmos. Res. 205, 60–69. https://doi.org/10.1016/j.atmosres.2018.02.006

12.I find the discussion section relatively weak, as certain findings lack sufficient reasoning or possible explanations. Furthermore, the biases in precipitation simulation are considered as a key limitation of this study. How big are the influences of these biases on your findings? Do you consider using bias-correction methods in the future studies?

-Answer: We sincerely appreciate your insightful comments. We agree that the discussion section can be further strengthened.

4 Discussion

Although earlier research has emphasized the necessity of analyzing extreme events under non-stationary conditions (Cheng et al., 2014; Byun and Hamlet, 2020; Liu et al., 2024), the

evolution of CCEs within a non-stationary climate framework remains poorly understood. Our study develops an innovative non-stationary framework integrating WRF-based dynamical downscaling with GAMLSS to reassess future recurrence risks of CCEs. The results reveal systematic underestimation of CCE frequencies by traditional stationary models, underscoring the critical need for time-varying risk assessments to avoid misleading projections and support robust climate adaptation strategies (Abdelmoaty and Papalexiou, 2023). This framework is transferable to other regions facing complex hydroclimatic interactions.

4.1 Dominance of hot extremes and temperature-driven shifts

The projected increase in CCEs, particularly under SSP5-8.5, aligns with global trends of intensifying hydroclimatic risks under continued warming (Asadieh and Krakauer, 2017; Zhang et al., 2021). Our findings indicate that hot-dry extremes dominate both spatially and temporally, increasing at 2.26 days per decade in summer under SSP5-8.5, while cold extremes decline. This pattern is consistent with studies highlighting the rising prevalence of hot-stagnation and hot-dry extremes in East Asia (Yin et al., 2025). The reversal between hot and cold extremes has been robustly linked to enhanced radiative forcing from anthropogenic greenhouse gas emissions (Samset et al., 2018; Kramer et al., 2021). Our analysis further reveals that temperature—not precipitation—is the primary driver of CCE changes in the MRB, as evidenced by the strong warming trend (0.46°C per decade under SSP5-8.5) alongside relatively stable precipitation (Fig. S2). This supports the hypothesis that thermodynamic effects, rather than dynamic ones, dominate mean-state changes in extremes (Horton et al., 2016; Van Der Wiel and Bintanja, 2021).

4.2 Non-stationarity: mean shifts outpace variability

A key advance of this study is the explicit detection of non-stationary characteristics in CCEs, which has been largely overlooked in prior compound event analyses. We find that under SSP5-8.5, 95.20% of grid cells exhibit non-stationarity, predominantly driven by changes in the Mn rather than Var, accounting for 80.81% of the transitions. This suggests that climate warming amplifies extremes primarily through shifts in baseline intensity—a thermodynamic effect—rather than through increased temporal variability. Similar findings have been reported at global scales, where mean warming dominates changes in extreme temperature distributions (Patel et al., 2024; Nordling et al., 2025). The spatial concentration of Mn-driven non-stationarity in downstream MRB and the Shaxi River Basin may reflect localized warming amplification due to urban heat islands or land-atmosphere feedbacks, a

phenomenon noted in other subtropical regions (Gao et al., 2018; Wu et al., 2020).

4.3 Frequency of recurrence systematically underestimated by stationary models

Our comparison between stationary and non-stationary models reveals that the latter captures a significant increase in recurrence risks, particularly for 100-year CCEs (3.12 days per decade under SSP5-8.5). Stationary models systematically underestimate these risks after 2045, consistent with global studies showing that conventional extreme value models fail to capture escalating severities under climate change (Feng et al., 2020; Xu et al., 2025). The stronger non-stationary response of 100-year events highlights the heightened vulnerability of high-impact, low-probability extremes—a critical insight for infrastructure design and disaster preparedness. The west-to-east gradient in recurrence risk, with hotspots in the Shaxi River Basin, may be attributed to topographic and land-surface heterogeneity, which modulate local hydroclimatic responses (Zheng et al., 2023; Zhang et al., 2025).

4.4 Methodological advances and limitations

Our integrated "bias-corrected CMIP6–WRF dynamical downscaling–GAMLSS" framework represents a significant methodological advancement over the direct use of raw GCM outputs or purely statistical downscaling for projecting CCEs. By resolving mesoscale circulations and explicitly simulating convective processes, our approach more faithfully captures the fine-scale spatiotemporal heterogeneity of precipitation and temperature fields in complex terrain, a capability that statistical methods, reliant on historically derived statistical relationships, fundamentally lack (Gutmann et al., 2012; Rahimi et al., 2024). Crucially, initializing the WRF model with a bias-corrected CMIP6 dataset mitigates the propagation and amplification of inherent GCM systematic errors, a strategy proven to enhance the credibility of regional climate projections (Zhang et al., 2024; Rahimi et al., 2024). Nonetheless, certain limitations persist. Even at convection-permitting resolution (3 km), the WRF model exhibits systematic biases in simulating orographic precipitation, a well-documented challenge often stemming from uncertainties in microphysical parameterization schemes and the representation of land-atmosphere energy and moisture exchanges over mountainous regions (Talbot et al., 2012; Zhang et al., 2025). Furthermore, while statistically robust, our current non-stationary GAMLSS framework employs time merely as a proxy covariate for climate change. This approach effectively detects and projects temporal trends in risk but falls short of elucidating the underlying physical drivers, such as the specific roles of evolving large-scale circulation patterns or soil moisture-atmosphere feedbacks. To overcome these constraints and solidify the

physical foundations of our projections, future work should focus on three promising avenues: first, explicitly embedding physical drivers like atmospheric circulation indices, antecedent soil moisture, or global mean temperature as covariates within the GAMLSS to establish a clearer causal chain from forcing to statistical response (Zeng et al., 2024; Ma et al., 2025); second, leveraging machine learning, such as convolutional neural networks, for the statistical post-processing of WRF outputs to correct systematic biases, or developing hybrid physics-informed machine learning models as a complementary approach to dynamical downscaling (Yin et al., 2021; Xie et al., 2023); and third, systematically quantifying the full cascade of uncertainty from GCMs through downscaling to statistical modeling, ideally through a super-ensemble of multiple CMIP6 models and WRF physical parameterizations, to provide probabilistic risk estimates crucial for informed decision-making.

References

Abdelmoaty, H.M., Papalexiou, S.M., 2023. Changes of Extreme Precipitation in CMIP6 Projections: Should We Use Stationary or Nonstationary Models? J. Climate 36, 2999–3014. https://doi.org/10.1175/JCLI-D-22-0467.1

Asadieh, B., Krakauer, N.Y., 2017. Global change in streamflow extremes under climate change over the 21st century. Hydrol. Earth Syst. Sci. 21, 5863–5874. https://doi.org/10.5194/hess-21-5863-2017

Byun, K., Hamlet, A.F., 2020. A risk-based analytical framework for quantifying non-stationary flood risks and establishing infrastructure design standards in a changing environment. J. Hydrol. 584, 124575. https://doi.org/10.1016/j.jhydrol.2020.124575

Cheng, L., AghaKouchak, A., Gilleland, E., Katz, R.W., 2014. Non-stationary extreme value analysis in a changing climate. Climatic Change 127, 353–369. https://doi.org/10.1007/s10584-014-1254-5

Feng, Y., Shi, P., Qu, S., Mou, S., Chen, C., Dong, F., 2020. Nonstationary flood coincidence risk analysis using time-varying copula functions. Sci. Rep. 10, 3395. https://doi.org/10.1038/s41598-020-60264-3

Gao, L., Huang, J., Chen, X., Chen, Y., Liu, M., 2018. Contributions of natural climate changes and human activities to the trend of extreme precipitation. Atmos. Res. 205, 60–69. https://doi.org/10.1016/j.atmosres.2018.02.006

Gutmann, E.D., Rasmussen, R.M., Liu, C., Ikeda, K., Gochis, D.J., Clark, M.P., Dudhia, J.,

Thompson, G., 2012. A Comparison of Statistical and Dynamical Downscaling of Winter Precipitation over Complex Terrain. J. Climate 25, 262–281. https://doi.org/10.1175/2011JCLI4109.1

Horton, R.M., Mankin, J.S., Lesk, C., Coffel, E., Raymond, C., 2016. A Review of Recent Advances in Research on Extreme Heat Events. Curr. Clim. Change Rep 2, 242–259. https://doi.org/10.1007/s40641-016-0042-x

Kramer, R.J., He, H., Soden, B.J., Oreopoulos, L., Myhre, G., Forster, P.M., Smith, C.J., 2021. Observational Evidence of Increasing Global Radiative Forcing. Geophys. Res. Lett. 48, e2020GL091585. https://doi.org/10.1029/2020GL091585

Liu, Y., Chen, J., Xiong, L., Xu, C.-Y., 2024. Integrating heterogeneous information for modeling non-stationarity of extreme precipitation in the Yangtze River Basin. J. Hydrol. 645, 132159. https://doi.org/10.1016/j.jhydrol.2024.132159

Ma, L., Hu, S., Zhou, B., Peng, J., Li, D., 2025. Novel dynamical indices for the variations of the South Asia high in a warming climate. Atmos. Res. 315, 107901. https://doi.org/10.1016/j.atmosres.2024.107901

Nordling, K., Fahrenbach, N.L.S., Samset, B.H., 2025. Climate variability can outweigh the influence of climate mean changes for extreme precipitation under global warming. Atmos. Chem. Phys. 25, 1659–1684. https://doi.org/10.5194/acp-25-1659-2025

Patel, R.N., Bonan, D.B., Schneider, T., 2024. Changes in the Frequency of Observed Temperature Extremes Largely Driven by a Distribution Shift. Geophys. Res. Lett. 51, e2024GL110707. https://doi.org/10.1029/2024GL110707

Rahimi, S., Huang, L., Norris, J., Hall, A., Goldenson, N., Risser, M., Feldman, D.R., Lebo, Z.J., Dennis, E., Thackeray, C., 2024. Understanding the Cascade: Removing GCM Biases Improves Dynamically Downscaled Climate Projections. Geophys. Res. Lett. 51, e2023GL106264. https://doi.org/10.1029/2023GL106264

Rahimi, S., Huang, L., Norris, J., Hall, A., Goldenson, N., Risser, M., Feldman, D.R., Lebo, Z.J., Dennis, E., Thackeray, C., 2024. Understanding the Cascade: Removing GCM Biases Improves Dynamically Downscaled Climate Projections. Geophys. Res. Lett. 51, e2023GL106264. https://doi.org/10.1029/2023GL106264

Samset, B.H., Sand, M., Smith, C.J., Bauer, S.E., Forster, P.M., Fuglestvedt, J.S., Osprey, S., Schleussner, C. -F., 2018. Climate Impacts From a Removal of Anthropogenic Aerosol Emissions. Geophys. Res. Lett. 45, 1020–1029. https://doi.org/10.1002/2017GL076079

Talbot, C., Bou-Zeid, E., Smith, J., 2012. Nested Mesoscale Large-Eddy Simulations with WRF: Performance in Real Test Cases. J. Hydrometeorol. 13, 1421–1441. https://doi.org/10.1175/JHM-D-11-048.1

Van Der Wiel, K., Bintanja, R., 2021. Contribution of climatic changes in mean and variability to monthly temperature and precipitation extremes. Commun. Earth Environ. 2, 1. https://doi.org/10.1038/s43247-020-00077-4

Wu, X., Hao, Z., Zhang, X., Li, C., Hao, F., 2020. Evaluation of severity changes of compound dry and hot events in China based on a multivariate multi-index approach. J. Hydrol. 583, 124580. https://doi.org/10.1016/j.jhydrol.2020.124580

Xu, W., Liu, Z., Gao, L., Lei, X., Zhang, Y., 2025. Changes in Global Marine Heatwaves in a Non-stationary Climate. Geophys. Res. Lett. 52, e2024GL114497. https://doi.org/10.1029/2024GL114497

Xie, Y., Sun, W., Ren, M., Chen, S., Huang, Z., Pan, X., 2023. Stacking ensemble learning models for daily runoff prediction using 1D and 2D CNNs. Expert Syst. Appl. 217, 119469. https://doi.org/10.1016/j.eswa.2022.119469

Yin, C., Ting, M., Kornhuber, K., Horton, R.M., Yang, Y., Jiang, Y., 2025. CETD, a global compound events detection and visualisation toolbox and dataset. Sci. Data 12, 356. https://doi.org/10.1038/s41597-025-04530-x

Yin, H., Zhang, X., Wang, F., Zhang, Y., Xia, R., Jin, J., 2021. Rainfall-runoff modeling using LSTM-based multi-state-vector sequence-to-sequence model. J. Hydrol. 598, 126378. https://doi.org/10.1016/j.jhydrol.2021.126378

Zeng, J., Zhang, S., Zhou, S., Obulkasim, O., Zhang, H., Lu, X., Dai, Y., 2024. Comparison of the risks and drivers of compound hot-dry and hot-wet extremes in a warming world. Environ. Res. Lett. 19, 114026. https://doi.org/10.1088/1748-9326/ad7617

Zhang, M., Han, Y., Xu, Z., Guo, W., 2024. Assessing Climate Extremes in Dynamical Downscaling Simulations Driven by a Novel Bias-Corrected CMIP6 Data. J. Geophys. Res.: Atmos. 129, e2024JD041253. https://doi.org/10.1029/2024JD041253

Zhang, W., Furtado, K., Wu, P., Zhou, T., Chadwick, R., Marzin, C., Rostron, J., Sexton, D., 2021. Increasing precipitation variability on daily-to-multiyear time scales in a warmer world. Sci. Adv. 7, eabf8021. https://doi.org/10.1126/sciadv.abf8021

Zhang, Y., Deng, C., Xu, W., Zhuang, Y., Jiang, L., Jiang, C., Guan, X., Wei, J., Ma, M., Chen, Y., Peng, J., Gao, L., 2025. Long-term variability of extreme precipitation with WRF

model at a complex terrain River Basin. Sci. Rep. 15, 156. https://doi.org/10.1038/s41598-024-84076-x

Zheng, M., Chen, X., Ruan, W., Yao, H., Gu, Z., Geng, K., Li, X., Deng, H., Chen, Y., Liu, M., 2023. Spatiotemporal variation of water cycle components in Minjiang River Basin based on a correction method for evapotranspiration products. J. Hydrol.: Reg. Stud. 50, 101575. https://doi.org/10.1016/j.ejrh.2023.101575

Minor Comments:

1.L29: Write out 3.55d/10a.

-Answer: Thank you for your valuable comment. We apologize for the incorrect expression of "3.55 d/10a." Following your suggestion, we will revise the manuscript and change all such expressions to "days per decade" in the revised version to ensure clarity and consistency.

2.L32: Define stationarity.

-Answer: Thank you for your suggestion. We will include a definition of stationarity in the revised manuscript as you recommended. Specifically, stationarity refers to the assumption that the statistical properties of a process, such as the mean, variance, and autocorrelation, do not change over time. In the context of climate and hydrological data, a stationary process implies that the distribution of climate variables remains constant throughout the time series, and the underlying parameters (such as mean and variance) do not exhibit long-term trends or shifts. We will clarify this definition in the revised manuscript.

3.L55: considering rephrasing the sentence into Therefore, traditional models fail to capture the non-stationary changes in these extreme events.

-Answer: Thank you for your suggestion. We agree with this expression and will rephrase the sentence as recommended in the revised manuscript.

4.In L71, the WRF model appears rather abruptly. Please introduce its relation with the RCMs.

-Answer: Thank you for your suggestion. We will enhance the explanation of the relationship between the WRF model and regional climate models (RCMs) in the revised manuscript to make it clearer and more coherent.

To overcome this constraint, dynamical downscaling, which utilizes nested high-resolution regional climate models (RCMs), provides a critical technical pathway to investigate climate response mechanisms at fine-scales (Tapiador et al., 2020; Rahimi et al., 2024). In this context, over the past decade, an increasing number of studies have begun to use RCMs to obtain high-resolution climate information. Bozkurt et al. (2019) used the Regional Climate

Model, version 4 (RegCM4), to evaluate the spatiotemporal variations of temperature and precipitation over the Pacific coast and the Andes Mountains. The results indicated that increasing the resolution effectively eliminates simulation errors caused by complex topography. McCrary et al. (2020) used multiple RCMs from the North American Coordinated Regional Downscaling Experiment (NA-CORDEX) to predict future snow changes in North America. They found that, particularly in high-elevation areas, the percentage of snow loss projected by GCMs was significantly higher than that projected by the RCMs. As an advanced convection-permitting RCM, the WRF model significantly enhances the simulation capability for meteorological processes at 1-10 km scales through its fully compressible, non-hydrostatic dynamic core framework (Talbot et al., 2012). This high-resolution simulation capability gives the WRF model a unique advantage in capturing small-scale meteorological phenomena. Zhou et al. (2024) developed a 9 km resolution regional reanalysis dataset covering the Tibetan Plateau based on the WRF model, and demonstrated its superior applicability compared to the fifth generation European Centre for Medium-Range Weather Forecasts Reanalysis (ERA5). Yang et al. (2025) revealed that the WRF model provides better accuracy in simulating snow depth during the cold season in high-elevation regions compared to ERA5-Land.

References

Bozkurt, D., Rojas, M., Boisier, J.P., Rondanelli, R., Garreaud, R., Gallardo, L., 2019. Dynamical downscaling over the complex terrain of southwest South America: present climate conditions and added value analysis. Clim. Dyn. 53, 6745–6767. https://doi.org/10.1007/s00382-019-04959-y

McCrary, R.R., Mearns, L.O., Abel, M.R., Biner, S., Bukovsky, M.S., 2022. Projections of North American snow from NA-CORDEX and their uncertainties, with a focus on model resolution. Climatic Change 170, 20. https://doi.org/10.1007/s10584-021-03294-8

Rahimi, S., Huang, L., Norris, J., Hall, A., Goldenson, N., Risser, M., Feldman, D.R., Lebo, Z.J., Dennis, E., Thackeray, C., 2024. Understanding the Cascade: Removing GCM Biases Improves Dynamically Downscaled Climate Projections. Geophys. Res. Lett. 51, e2023GL106264. https://doi.org/10.1029/2023GL106264

Talbot, C., Bou-Zeid, E., Smith, J., 2012. Nested Mesoscale Large-Eddy Simulations with WRF: Performance in Real Test Cases. J. Hydrometeorol. 13, 1421–1441. https://doi.org/10.1175/JHM-D-11-048.1

Tapiador, F.J., Navarro, A., Moreno, R., Sánchez, J.L., García-Ortega, E., 2020. Regional

climate models: 30 years of dynamical downscaling. Atmos. Res. 235, 104785. https://doi.org/10.1016/j.atmosres.2019.104785

Yang, T., Chen, X., Hamdi, R., Li, L., Cui, F., De Maeyer, P., Duan, W., 2025. Rainfall-Driven Extreme Snowmelt Will Increase in the Tianshan and Pamir Regions Under Future Climate Projection. J. Geophys. Res.: Atmos. 130, e2024JD042323. https://doi.org/10.1029/2024JD042323

Zhou, P., Tang, J., Ma, M., Ji, D., Shi, J., 2024. High resolution Tibetan Plateau regional reanalysis 1961-present. Sci. Data 11, 444. https://doi.org/10.1038/s41597-024-03282-4

5.Similarly, in L78, please add how GAMLSS and WRF fit in here. While introducing the objective of this paper, the authors should mention what types of CCEs they are looking into.

-Answer: Thank you for your comment. We perform dynamical downscaling using the WRF model to downscale the bias-corrected CMIP6 data (1.25° × 1.25°) to a 3 km resolution. Subsequently, compound extreme climate events (CCEs) are calculated based on the high-resolution WRF outputs. These calculated CCEs are then used as input for the GAMLSS framework to analyze their non-stationary characteristics. This approach allows the integration of high-resolution dynamical downscaling with the statistical modeling of extremes, ensuring that both local-scale variability and non-stationarity are adequately captured. We will provide a more detailed description of this method in the revised manuscript. In addition, based on your suggestion, we will mention the four types of CCEs (hot-wet events, hot-dry events, cold-wet events, and cold-dry events) in the introduction section.

6.Please add references to support the statement 'complex interactions between topography and climate give rise to high-intensity compound hydroclimatic extremes.' (L81-82).

-Answer: We focus on the Minjiang River Basin (MRB), a subtropical monsoon-dominated basin of southeastern China, where complex interactions between topography and climate give rise to high-intensity compound hydroclimatic extremes ***(Gan et al., 2025; Geng et al., 2024; Wang et al., 2024)***.

References

Gan, B., Liu, M., Cui, H., Chen, X., Chen, Y., Gao, L., Deng, H., 2025. Spatiotemporal patterns and propagation of meteorological and hydrological drought in a humid basin of Southeast China. Sci. Rep. 15, 31720. https://doi.org/10.1038/s41598-025-17005-1

Geng, K., Chen, X., Zheng, M., Gao, Y., Gu, Z., Yao, H., 2024. The influence of human activities on rainfall-runoff relationships at different time scales in the Minjiang River

Basin. Theor. Appl. Climatol. 155, 8435–8454. https://doi.org/10.1007/s00704-024-05124-0

Wang, S., Chen, X., Yao, H., Ruan, W., Gu, Z., Li, X., Chen, Y., Liu, M., Deng, H., 2024. Separation and spatial variations of typhoon and non-typhoon rainfall at different timescales in typical region of southeast China. Intl. J Climatol. 44, 4611–4628. https://doi.org/10.1002/joc.8599

7.Define non-stationarity detection (L85).

-Answer: Thank you for your suggestion. We will include a definition of non-stationarity detection in the revised manuscript as you recommended. Non-stationarity detection refers to the identification of changes in the statistical properties of a time series over time, indicating that the process is no longer stationary. This may include shifts in the mean, variance, or autocorrelation, as well as changes in the underlying distribution or trend of the data.

8.L109, write out ERA5 if it is the first use.

-Answer: Thank you for your comment. We will make sure to address this issue and provide the full name of ERA5 (the fifth generation European Centre for Medium-Range Weather Forecasts Reanalysis) when it is first mentioned in the revised manuscript.

9.Provide the names and associated details of the 18 models used in your dataset.

-Answer: Thank you for your suggestion. We will provide a list of the 18 models used in the bias-corrected CMIP6 dataset (Xu et al., 2021) in the supplementary file as requested.

Table S1 CMIP6 models used in CMIP6bc.

No.	Model	Institution	Approximate grid spacing
1	ACCESS-CM2	Commonwealth Scientific and Industrial Research Organisation (Australia)	1.875° × 1.25°
2	ACCESS-ESM1–5	Commonwealth Scientific and Industrial Research Organisation (Australia)	1.875° × 1.25°
3	CanESM5	Canadian Centre for Climate Modelling and Analysis (Canada)	2.81° × 2.81°
4	BCC-CSM2-MR	Beijing Climate Center (China)	1.125° × 1.125°
5	FGOALS-f3-L	Institute of Atmospheric Physics, Chinese Academy of Sciences (China)	1.25° × 1°
6	FGOALS-g3	Institute of Atmospheric Physics, Chinese Academy of Sciences (China)	2° × 2.25°
7	EC-Earth3	European EC-Earth Consortium (Europe)	0.70° × 0.70°
8	EC-Earth3-Veg	European EC-Earth Consortium (Europe)	0.70° × 0.70°
9	IPSL-CM6A-LR	Institute Pierre Simon Laplace (France)	2.5° × 1.26°
10	AWI-CM-1-1-MR	Alfred Wegener Institute, Helmholtz Centre for Polar and Marine Research (Germany)	0.94° × 0.94°
11	MPI-ESM1-2-HR	Max Planck Institute for Meteorology (Germany)	0.94° × 0.94°
12	MPI-ESM1-2-LR	Max Planck Institute for Meteorology (Germany)	1.875° × 1.875°
13	MIROC6	Japan Agency for Marine-Earth Science and Technology (Japan)	1.41° × 1.41°
14	MRI-ESM2-0	Meteorological Research Institute, Japan Meteorological Agency (Japan)	1.125° × 1.125°
15	NorESM2-LM	Norwegian Climate Center (Norway)	2.5° × 1.875°
16	CESM2	Climate and Global Dynamics Laboratory, National Center for Atmospheric Research (USA)	1.25° × 0.94°
17	CESM2-WACCM	Climate and Global Dynamics Laboratory, National Center for Atmospheric Research (USA)	1.25° × 0.94°
18	GFDL-ESM4	Geophysical Fluid Dynamics Laboratory, National Oceanic and Atmosphere Administration (USA)	1.25° × 1.0°

References

Xu, Z., Han, Y., Tam, C.-Y., Yang, Z.-L., Fu, C., 2021. Bias-corrected CMIP6 global dataset for dynamical downscaling of the historical and future climate (1979–2100). Sci. Data 8, 293. https://doi.org/10.1038/s41597-021-01079-3

10.In Fig. 2, please consider using another color for the meteorological stations as they are sometimes hard to tell due to the elevation data.

-Answer: Thank you for your suggestion. We will modify the manuscript accordingly and use a different color for the meteorological stations in the revised version to avoid confusion with the elevation data (Fig. 2).

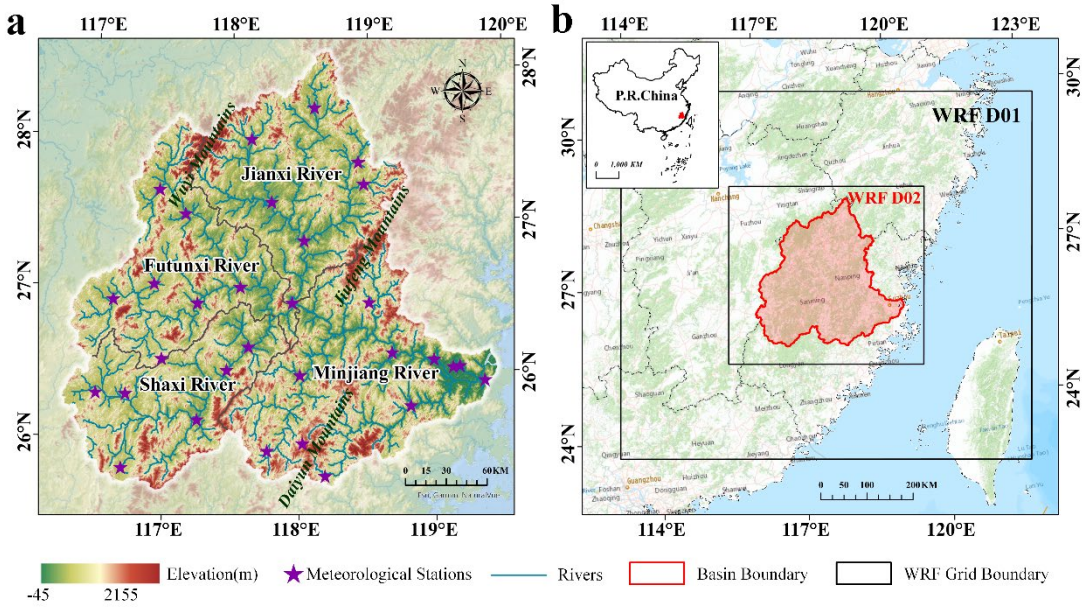

Fig. 2. Study area and model configuration. (a) Topographic features of the MRB (m) and (b) Model configuration with 9-km (D01) and 3-km (D02) nested domains (Zhang et al., 2025). Basemap source: © Esri, https://services.arcgisonline.com

References

Zhang, Y., Deng, C., Xu, W., Zhuang, Y., Jiang, L., Jiang, C., Guan, X., Wei, J., Ma, M., Chen, Y., Peng, J., Gao, L., 2025. Long-term variability of extreme precipitation with WRF model at a complex terrain River Basin. Sci. Rep. 15, 156. https://doi.org/10.1038/s41598-024-84076-x

11.When referring to the figures, please use Fig. instead of Figure to make sure it is consistent with the captions.

-Answer: We sincerely appreciate your valuable comments, and we apologize for the inconsistency in referring to the figures. Following your suggestion, we will ensure format consistency in the revised manuscript to align with the figure captions. Thank you once again for your careful review and valuable suggestions.